

EFFECT OF PRESSURE AND WATER SATURATION ON
PERMEABILITY OF WESTERN TIGHT SANDSTONES

By

A. P. Byrnes, K. Sampath, P. L. Randolph
Institute of Gas Technology
3424 South State Street
Chicago, Illinois 60616

ABSTRACT

The Institute of Gas Technology (IGT) is conducting tests on the effect of pore and confining pressure on the absolute and relative permeability of Western tight sandstone. Cores from the Canyon Largo No. 256 Well in the San Juan Basin, Dakota Formation, Farmington, New Mexico, and the Mobil F31-13G Well in the Piceance Basin, Zones 3 and 6, Rio Blanco County, Colorado, are being examined.

Steady state flow and pressure pulse decay tests have been conducted at pore pressures up to 4700 psi and confining pressures up to 9700 psi. Relative gas permeability values have been measured at different levels of water saturation and compared with an earlier empirical correlation proposed by Corey.

The effect of confining pressure on tight sandstone was studied and results were found to conform to the observations of earlier investigators.

INTRODUCTION

In many natural gas producing areas, technology for conventional exploration is sufficiently advanced that the analysis of wireline logs provides conclusive information as to whether or not production rates will be sufficient to warrant cementing of production casing and well completion. In such areas, the cost of an abandoned, unsuccessful exploratory well is often less than half the cost of a well placed in commercial production. In the Western tight sands, however, cementing of production casing, perforating, and production testing are essential aspects of definitive exploratory well evaluation because current technologies are not adequate to evaluate producing capability without production testing. Research is required to fully understand the factors controlling effective in situ permeability and to improve wireline logging and interpretation technology.

This report describes IGT research on core from two wells. The samples of Dakota Formation from the San Juan Basin Well Canyon Largo No. 256 were selected to permit comparison with similar, but unpublished, measurements by

Mr. Rex Thomas at the Bartlesville Energy Technology Center. The second well is the Mobil F31-13G Well in the Piceance Basin. This well is being tested by Mobil Oil Company/DOE. It is doubtful whether the core samples provided to IGT are representative of the sandstones actually tested.

Laboratory studies on core from tight sands wells have revealed that permeability to natural gas is a strong function of both confining pressure on the rock and the fractional saturation of the pores with formation waters. Procedures used in these studies assumed that permeability is dependent only on the effective stress or net confining pressure, which is the difference between the confining pressure and the pore pressure, irrespective of the absolute values of these pressures. The strong dependence of tight sandstone permeability on net confining pressure has been well documented by previous investigators.^{1,2,3,4}

Permeability of a porous medium is calculated using the Darcy Equation for fluid flow. Evaluation of gas permeabilities involves a correction due to "gas slippage," as proposed by Klinkenberg.⁵ The Klinkenberg correlation predicts a linear dependence of permeability on reciprocal mean pressure for higher permeability porous media. The applicability of this correlation to tight sandstones is under investigation.

The relative permeability to gas of a rock partially saturated with water has been found to be independent of the variation of permeability with confining pressure.^{4,6} Partial water saturation achieved by laboratory evaporation techniques was assumed to adequately reproduce water distribution under reservoir conditions in this work.

This study is the first report of our data derived from experiments designed to evaluate the validity of some of the assumptions involved in the determination of in situ tight sandstone permeability.

APPARATUS AND EXPERIMENTAL METHODS

A schematic diagram of the experimental apparatus is shown in Figure 1. Cylindrical cores 1 inch in diameter by 2 inches long were cut parallel to the bedding plane, and the ends were cut off with a precision diamond saw using 60,000 ppm NaCl solution. End pieces cut off the core plug used for permeability study were used for rock description including mercury capillary pressure injection test, pore size distribution analysis, x-ray diffraction, scanning electron microscopy, and rock thin section petrography.

The cores were dried in a vacuum oven at 90°C and less than 1 psi for more than 3 days and then weighed. It was observed that heating the cores for longer periods of time did not affect the permeability or the dry weight. After drying at temperatures of 115°C, however, lower dry weights and permeabilities higher by approximately 33% were measured. The initial permeability values were regained by saturation with NaCl solution and reheating at 90°C. This behavior is probably due to dehydration of clays and removal of adsorbed water.⁷ Cores exposed to room air adsorbed water that resulted in a gain of up to 6% water saturation in the pores although no significant permeability change was measured.

The cores and grooved stainless steel end plugs were placed in a 3/8-inch thick rubber sleeve in a cell capable of exerting up to 10,000 psi hydrostatic confining pressure, using water, and capable of flowing gas or liquid at fluid pressures up to 5000 psi.

Because of the strong dependence of permeability of tight sandstone on confining pressure, a high differential pore pressure across the core can result in a large net confining pressure gradient and, in turn, a large change in permeability from the core inlet to the core outlet. For this reason, differential pressures were held below 60 psi. Confining pressures were generated using a pneumatically controlled liquid pump and pore pressures were generated up to 5000 psi using a gas booster. To control differential pressures from 1-60 psi at up to 5000 psi, a pneumatically controlled micrometering back pressure control valve was used. This valve controlled the drop in pressure from within the system to the atmospheric pressure flow meter. With an upstream volume of 700 cc and a downstream volume of 350 cc with respect to the core, it was found that total system pore pressure did not change during a permeability measurement by more than 10 psi. This permitted steady state flow measurements to be performed at high pressures with negligible change in the effective stress on the core. The confining pressure and fluid pressures were measured using pressure gauges (.1% accuracy), and the differential pressure at all fluid pressures was measured using a sensitive differential pressure transducer ($\pm .05$ psid). The transducer output was recorded continuously during all experiments.

Flow rates were measured either by horizontal displacement of a meniscus in a capillary or by displacement of water from a column. Both methods were found to agree within 1% and to be sensitive to changes in differential pressures of less than .1 psid at all fluid pressures. At low pore pressures, a small volume tube was connected from the downstream end plug directly to the flow meter. At high pore pressures, a small volume tube was connected from the outlet of the micrometering back pressure control valve to the flow meter.

Low pore pressure permeabilities were measured using N_2 gas at initial confining pressures of 120 psi above mean pore pressure (one-half the sum of upstream and downstream pressure). Confining pressure was then increased to 520, 1020, 2020, 3020, 4020, 5020, and 6020 psi with dry N_2 introduced at a constant pressure of 40 psi to the upstream end of the core. The downstream end of the core was maintained at ambient pressure. Klinkenberg extrapolations were determined at 120 psi net confining pressure in general using differential pressures of 5, 15, and 50 psi. When confining pressure was increased, equilibrium was reached within 1 to 2 hours. Equilibrium was assumed when flow rates remained constant within 1-2% over an interval of 15 minutes.

High pore pressure permeability was measured using both steady state and pressure pulse decay methods. Steady state permeability was determined at differential pressures of 5, 15, and 50 psi at increasing mean pore pressures of near atmospheric up to reservoir pressure. Confining pressure was maintained at 120 psi greater than pore pressure. While pore pressure was being increased, the net confining pressure was never permitted to exceed 120 psi to avoid hysteresis effects. Immediately following a steady state test pressure pulse decay tests were performed. To do this, the system was shut in and pressures upstream and downstream of the core were allowed to equilibrate.

A pressure approximately 50 psi higher than the pore pressure was generated in the vessels upstream of the core and then, by opening the upstream valve, a differential pressure was instantly induced across the core. By monitoring the upstream pressure decay as a function of time, permeability was calculated.

Cores used in relative permeability studies were first subjected to a vacuum (< 0.1 psia) for 2 hours. The vacuum chamber was filled with a solution of NaCl (15 g/lt). The cores then remained immersed in the brine for 12 hours before measuring permeability. Porosities determined by water saturation were consistently lower than porosities determined by mercury injection. The difference in porosities was within the API requirements (± 0.5 porosity percent), but the porosity values affected the determination of water saturation significantly. Since the mercury injection method does not account for immobile water adsorbed by the clays in the rock, porosities determined using water saturation were used to calculate fractional water saturation. Water from the cores was permitted to evaporate at atmospheric conditions to lower partial water saturations, determined by weight. The cores were then placed within the cell. A period of about 2 hours was permitted to elapse to allow redistribution of water throughout the pores by capillary pressure. Subsequently, gas was flowed at 40 psid, with 120 psi net confining pressure. After testing, the core was reweighed to confirm that the water saturation had not changed during the experiment.

Initial permeability to gas was redetermined after heating the core in a vacuum oven at 90°C . In some cases, permeability was decreased, but not significantly.

RESULTS AND DISCUSSION

Effect of Rock Stress on Permeability to Gas

In an actual reservoir, local depositional and tectonic stresses add components of stress in unknown directions. Because the exact nature of in situ stresses is unknown, studies have been performed under hydrostatic conditions.

Core numbers (depth-ft), mercury-determined porosity, and gas permeability for different net confining pressures (overburden pressure) at constant low pore pressure (40 psi inlet) are shown in Table 1 and Figure 2. Under increasing confining pressures, permeability is reduced as much as 50 to 60 percent at a net confining pressure of 1000 psi and as much as 95 percent at 5000-6000 psi. These trends agree with previous studies on core from different tight sands areas and from previous studies on core from the Mobil F31-13G Well.⁸

Figure 3 illustrates the extreme sensitivity of permeability to net confining pressure at low confining pressures. Permeability values obtained from routine measurements appear to be of dubious value in view of the extreme sensitivity to confining pressure. A more extensive study of tight sandstones found a correlative relation between confining pressure and permeability above 2000 psi confining pressure, but no correlation between permeability and reduction due to confining stress was found which extended down to the 150-250 psi range.⁹

Tight sandstones exhibit a stronger dependence on net confining pressure than higher permeability rocks do.¹ This behavior has been attributed to differences in the ratio of cross-sectional area to the circumference of pores.¹ Further, fractures and shale streaks have a strong effect on permeability reductions in tight sands.^{3,4} Significantly different pore geometry may be involved in the observed differences in behavior. Recent scanning electron microscope studies of pore casts¹⁰ indicate that unlike coarse grained sands which contain more tubular pores, tight sands have pore spaces connected by oblong tabular pores. Jones and Owens⁹ have found that flow through cores from the Frontier, Mesaverde, and Cotton Valley formations can best be modeled by flow through ducts or slits.

Hysteresis of permeability results from stress induced on a core, and the extent of hysteresis is a function of the maximum stress to which the core has been subjected.^{2,3} Hysteresis effects observed by IGT are shown in Figure 4. Initial permeability was regained by the stressed cores only after approximately 2 weeks at 90°C or 3 to 6 weeks at atmospheric conditions. Similar response has been observed for other tight sandstones as well.⁴

After initial permeability had been regained, cores exhibited nearly the same reduction in permeability with increasing confining pressure as was observed on initial testing (Figure 5).

The gas permeability, as mentioned earlier, was determined by measuring the gas flow rate q through the core. From Darcy's Equation,

$$K = \frac{\mu L}{A(\Delta P)} q$$

$$K_g = \frac{2\mu L P_b}{A(P_1^2 - P_2^2)} Q \quad (\text{where } Q \text{ is measured flow rate at pressure } P_b)$$

At low pore pressures, permeabilities were measured at different differential pressures across the core while the downstream end of the core was maintained at atmospheric pressure. This, in effect, yielded permeability values at different mean pore pressures and these were used in the Klinkenberg extrapolations. An example of the results are presented in Figure 6 for Mobil F31-13G core No. 8498. Similar results were found for the other cores.

At higher pore pressures, mean pore pressure changes very little with changes in the relatively low differential pressures maintained across the cores. Flow rates measured at varying differential pressures indicate that, contrary to what might be expected from Darcy's Equation, a plot of Q versus $(P_1^2 - P_2^2)$ yields a non-zero intercept (Figure 7). Similar behavior has been observed by other investigators, who found that the slope of the line obtained by plotting flow rate versus differential pressure did not have a constant slope. Since the points exhibited a good linear fit (with regression coefficients > 0.97), permeability was calculated from the slope of this line. Permeabilities calculated from flow rates measured at only one differential pressure would be proportional to the slope of the line connecting the origin to the point value on a Q versus $(P_1^2 - P_2^2)$ plot. Since the observed intercepts were positive, permeabilities calculated from the slope of the line are lower than those that would be obtained from point measurements made at a single differential pressure.

Reasons for the observed deviation are unknown at present.

Following each series of steady state tests at a certain pore pressure, a pressure pulse decay test was performed. Bruce et al. (1968)¹¹ showed, by analogy with electrical systems, that permeability can be determined by imposing a pressure pulse upstream of the core and monitoring the pressure decay caused by flow through the core to a downstream closed chamber. The relevant equation is

$$(P_1 - P_f)_t = (P_1 - P_f)_{t=0} \frac{V_2}{V_1 + V_2} e^{-\alpha t}$$

where

$$\alpha = \frac{KA}{\mu BL} \frac{V_1 + V_2}{V_1 V_2}$$

It is then possible to solve for K:

$$K = \frac{\alpha \mu BL}{A} \frac{V_1 V_2}{V_1 + V_2}$$

Using previously measured values for μ , B, L, A, V_1 , V_2 and from the pressure decay data, assumptions made in this approach are -

- 1) Darcy's law is valid
- 2) Fluid flow is laminar
- 3) Viscosity and compressibility are constant for the whole system
- 4) The pore volume is small compared to the upstream and downstream volumes.

Figure 6 shows a Klinkenberg extrapolation for core No. 8498 using low pore pressure data at 120 psi net confining pressure. The extrapolation has a close linear fit up to 1000 psia mean pore pressure. In view of the assumptions involved in the Klinkenberg correlation, the measured permeability data appears to exhibit a reasonable linear dependence on reciprocal mean pressure. However, at high pore pressures, the slope increases sharply resulting in a lower extrapolated permeability. This is shown with an expanded scale in Figure 8 for both steady state and pressure pulse decay determined permeabilities. Similar results were found for other cores. This behavior may result from the questionable significance of permeability measurements with only 120 psi net confining pressure, deviations from the effective stress assumption as pore pressure is increased, or changes in gas flow behavior at high pore pressure as predicted by Klinkenberg.

WATER SATURATION EFFECTS

Cores were saturated with 15g/lit NaCl solution, and permeabilities were determined at 120 psi net confining pressure with 40 psi inlet pressure. Measured values were only 5-15% of the Klinkenberg extrapolated permeabilities measured at the same net confining pressure. However, permeability measurements were complicated by decreases in permeability with time, presumably due to clay fines displacement causing blockage of pores. Reversal of flow direction for core F31-13G No. 9957 resulted in an increase in measured

permeability up to approximately 20% of the Klinkenberg extrapolated value followed by a decrease down to approximately 10% until flow direction was reversed again. For some cores, flow rate continued to decrease until no flow was detected. For core No. 8498A, no significant fines displacement was noted and brine permeability was approximately 36% of the low pore pressure Klinkenberg extrapolated gas permeability and 57% of the high pore pressure extrapolation. Jones and Owens⁹ determined that salt solution with concentrations as high as 60,000 ppm cause permeability reductions similar to those observed here. Subsequent use of fresh water caused a minor decrease in permeability indicating that the salt solution had been nearly as damaging to the core as fresh water would have been. After redrying at 90°C, cores regained approximately the same gas permeability as was measured before the liquid flow tests.

Scanning electron micrographs presented further on indicate the limited extent of rock-fluid interaction and the presence of only small quantities of expanding clays. It thus appears that the significant reduction in brine permeability has to be attributed to a different mechanism.

Relative gas permeability was measured using the stationary liquid method. Different levels of water saturation were attained by evaporation of water from a saturated core. Figure 9, 10, 11, and 12 show the effect of partial water saturation on gas permeability at 120 psi net confining pressure. Figures 10 and 11 also show the results of relative permeability measurements on core plugs cut from adjacent locations on cores No. 8498 and No. 9998. The relative gas permeability behavior of the different core plugs appears to be similar. Figure 12 shows results of two different relative permeability measurements on core No. 9957. The higher values were obtained after the core had been dried at 115°C. These curves are similar to those obtained in similar experimental methods.⁴

Corey,¹² incorporating previous work by Purcell¹³ and Burdine¹⁴ based upon capillary pressure description of rock pores, developed an empirical equation that describes the decrease in gas relative permeability with increasing fractional water saturation:

$$K_{rg} = \left[1 - \frac{S_w - S_{wc}}{1 - S_{gc} - S_{wc}} \right]^n \left[1 - \left[\frac{S_w - S_{wc}}{1 - S_{wc}} \right]^2 \right]$$

In the original formulation the value 2 was used for n. Tight sands reservoirs are capable of being approximately characterized by this equation using values of $S_{wc} = 0$, $S_{gc} = .2-.3$, and $n = 1.1-1.3$. Corey Equation fits are shown on Figures 9, 10, 11, and 12 with the constants used. The relationship between the values for m used in tight sands and the theoretical approach used by Burdine is still being studied. Its use as a rough tool given routine determinations of water saturation are, however, useful for engineering approximations until detailed core analysis is possible. Use of water saturation as determined by routine core analysis requires that the effect of coring operations, including fluid invasion, water expulsion by gas expansion in pores on depressurization, and surface handling on fluid saturations must be understood. For tight sands, none of these have been evaluated analytically and therefore fluid saturations, as measured, are suspect.

Rock Description

Fundamental to understanding fluid flow through porous media is understanding the nature of the porous media itself. On all cores studied, an attempt was made to understand basic characteristics of the rock, including pore size distribution, capillary pressures, mineralogy, cementing, lithology, pore geometry, and more importantly to tight sandstones, clay morphology and distribution. The number of samples studied is not yet large enough to establish meaningful correlations.

Capillary pressure curves and related pore size distribution are shown in Figure 13. No strong relationship is apparent between pore size distribution and rock behavior under stress. However, in general, as might be expected, cores exhibiting the highest permeability also exhibited the presence of a greater percentage of large pores. It was found that sample size for mercury injection tests can have a dramatic effect on the capillary pressure curve produced (see Figures 13 and 14). Finer samples or samples broken during sizing operation develop increased numbers of large pores (Figure 14). The straight line segments in Figure 14 are the result of about 15 data points per curve.

Figure 15 shows the blockage of pores by intergrown clays for the Canyon Largo No. 256 core. Increased magnification shows the extremely fine morphology of the illite and illustrates the extent to which tortuosity of fluid flow through intergrown areas is increased (Figure 16). Because of the fineness of the clays dislodging of particles and subsequent blockage of pores is easily caused by liquid flow. Figure 17 shows illite clays morphology for F31-13G core No. 9957. After immersion in 60,000 ppm NaCl solution, fine clays are still apparent, but some dissolution and cementing has resulted (Figure 18).

CONCLUSIONS

Gas permeability measurements at varying confining pressures confirm the strong dependence of tight sandstone permeability on confining pressure. High pore pressure measurements indicate that gas permeabilities are reduced at higher pressures. Also, departures from Darcy's law that are not yet understood were observed for pore pressures in excess of 500 psi (as illustrated herein for core from 8498 feet in Mobil's PCU F31-13G Piceance Basin well.)

A strong decrease in effective gas permeability with increasing partial water saturation was observed. An empirical fit of the Corey Equation indicated that, for the tight sands studied, the curves could be described when using the equation

$$K_{rg} = \left[1 - \frac{S_w - S_{wc}}{1 - S_{gc} - S_{wc}} \right]^n \left[1 - \left[\frac{S_w - S_{wc}}{1 - S_{wc}} \right]^2 \right]$$

with $n = 1.1-1.3$, $S_{gc} = .2-.3$, and $S_{wc} = 0$.

The presence of fine grained clays intergrown across pore entries and clay cementing appear to have reduced the permeability of cores from both areas studied. Clays were found to be sensitive to even high salinity solutions. Liquid flow resulted in fines displacement and blockage of pores thereby reducing permeability significantly. Permeability to brine was lower

than the value obtained using the Klinkenberg extrapolations for each of the cores.

The high pressure tests were performed under conditions closer to those in the reservoir. More tests need to be performed to compare high pressure gas flow with liquid flow. The technique used for achieving partial water saturation needs to be evaluated with respect to its effect on relative permeability. The effect of the magnitude of the differential pressure imposed across the core on the measured permeability value needs to be examined.

NOMENCLATURE

- α = slope of semi log plot of P_1 versus time
- β = compressibility, psia^{-1}
- μ = viscosity, cp
- A = cross-sectional area, cm^2
- K = permeability, md
- K_g = effective gas permeability, md
- L = length, cm
- m = slope of line
- n = exponent in Corey Equation, subscripts 1, 2, b indicate upstream and downstream of the core, respectively
- P = pressure, psia
- P_m = mean pore pressure $(P_1 + P_2/2)$, psia
- Q = flow rate, cm^3/s
- R^2 = linear regression coefficient, values close to 1.00 indicate best fit
- S_{gc} = critical or irreducible gas saturation
- S_w = water saturation in pores
- S_{wc} = critical or irreducible water saturation
- V = volume, cm^3
- Z = gas compressibility factor

REFERENCES

1. Fatt, I., Davis, D. H., "Reduction in Permeability with Overburden Pressure," Trans. AIME (1952), Tech. Note 147, 194, 329.
2. McLatchie, A. S., Hemstock, R. A., Young, J. W., "The Effective Compressibility of Reservoir Rock and Its Effect on Permeability," J. Pet. Tech. (June 1958), 49-51.
3. Vairogs, J. Hearn, C. L., Dareing, D. W., Rhoades, V. W., "Effect of Rock Stress on Gas Production from Low Permeability Rocks," J. Pet. Tech. (1971), 1161-1167.
4. Thomas, R. D., Ward, D. C., "Effect of Overburden Pressure and Water Saturation on Gas Permeability of Tight Sandstone Cores," J. Pet. Tech. (February 1972), 120-124.
5. Klinkenberg, L. J., "The Permeability of Porous Media to Liquids and Gases," (API 11th Mid-Year Meeting, Tulsa, Oklahoma, May 1941) Drill Prod. Practice (1941), 200-213.
6. Fatt, I., "The Effect of Overburden Pressure on Relative Permeability," Trans. AIME, (1952), Tech. Note 194, 198, 325-326.
7. Bush, D. C., Jenkins, R. E., "Proper Hydration of Clays for Rock Property Determinations," J. Pet. Tech (July 1970), 800-804.
8. Fitch, J. L., "Demonstration of Massive Hydraulic Fracturing Mesaverde Formation, Piceance Basin, Colorado," Proc. Third ERDA Symposium on Enhanced Oil and Gas Recovery, Tulsa, August 30-September 1, 1977. p E 3/1-3/11.
9. Jones, F. O., Owens, W. W., "A Laboratory Study of Low Permeability Sands," SPE 7551, 1979 SPE Symposium on Low Permeability Gas Reservoirs, May 20-22, Denver, p 325-334.
10. Grunberg, L., Nissan, A. H., "The Permeability of Porous Solids to Gases and Liquids," J. Inst. Pet. (August 1943) 29, 236, 193-225.
11. Brace, W. F., Walsh, J. B., Frangos, W. T., "Permeability of Granite Under High Pressure," J. Geophys. Res. (March 1968), 73, 6, 2225-2236.
12. Corey, A. T., "The Interrelation Between Gas and Oil Relative Permeabilities," Prod. Monthly (November 1954), 38-41.
13. Purcell, W. R., "Capillary Pressures - Their Measurement Using Mercury and The Calculation of Permeability Therefrom," Trans AIME (February 1949), 39-48.
14. Burdine, N. T., "Relative Permeability Calculations from Pore Size Distribution Data," Trans. AIME (1953), 198, 71-78.

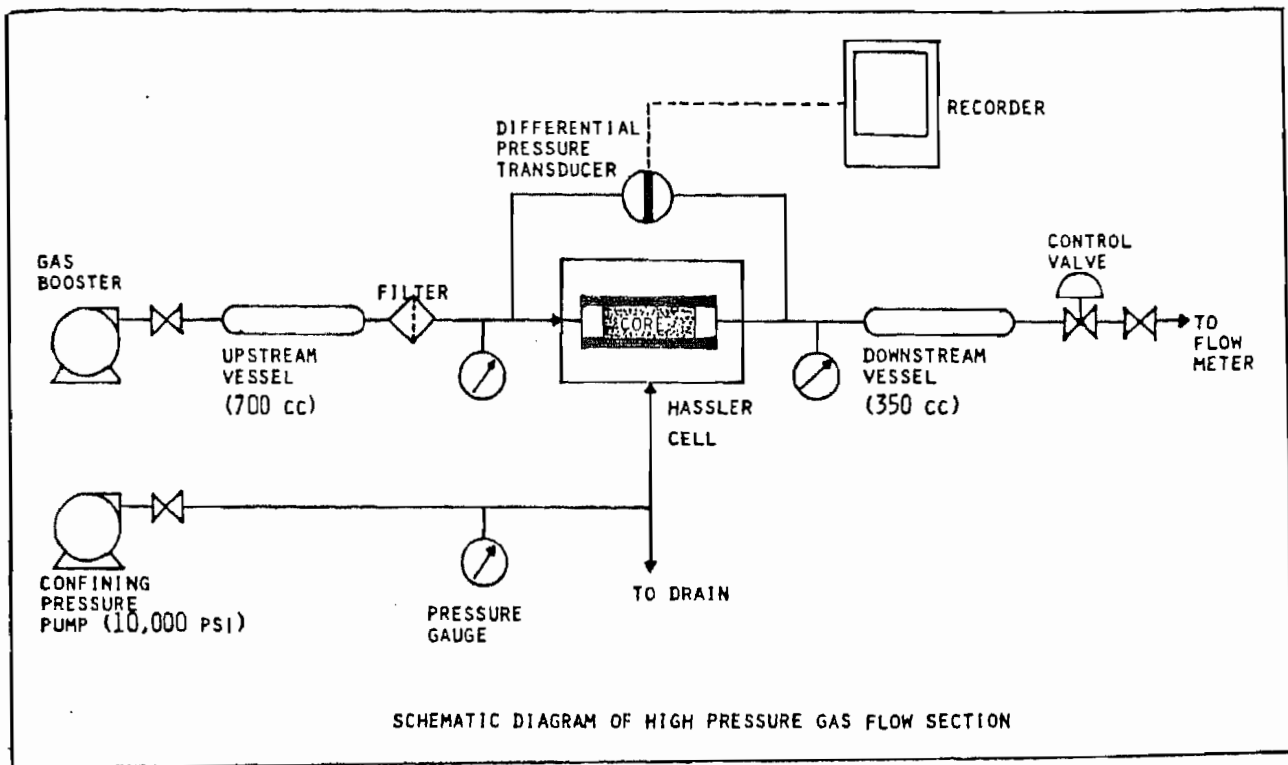


FIGURE 1

Table 1. EFFECT OF OVERBURDEN PRESSURE ON INITIAL GAS PERMEABILITY

Canyon Largo #256 Core #	Mercury Porosity (%)	K* (md)	% Initial Permeability At Overburden Pressures						
			500	1000	2000	3000	4000	5000	6000
6949	7.3	.042	59.4	31.9	18.3	11.2	6.9	4.6	3.6
7011	11.0	.067	38.8	29.9	22.4	17.9	13.3	7.7	3.6
7011H		.035	25.0	19.4	14.1	11.2	7.4	6.9	3.6
7103	6.9	.047	--	26.2	12.7	7.1	6.0	2.6	--
PCU 31-13									
Core #									
8498	6.4	.027	43.8	34.4	23.0	13.3	8.9	5.5	
9957	9.5	.110	53.9	47.7	28.7	18.4	12.7	9.7	
9957H		.055	34.1	24.7	16.0	12.2	10.3	9.7	
9998	7.3	.029	48.7	41.0	27.0	17.8	14.2	10.2	

H - Hysteresis test data. Percentages listed are of initial unstressed permeability.

* Permeability at 40 psi inlet pressure and 140 psi confining pressure.

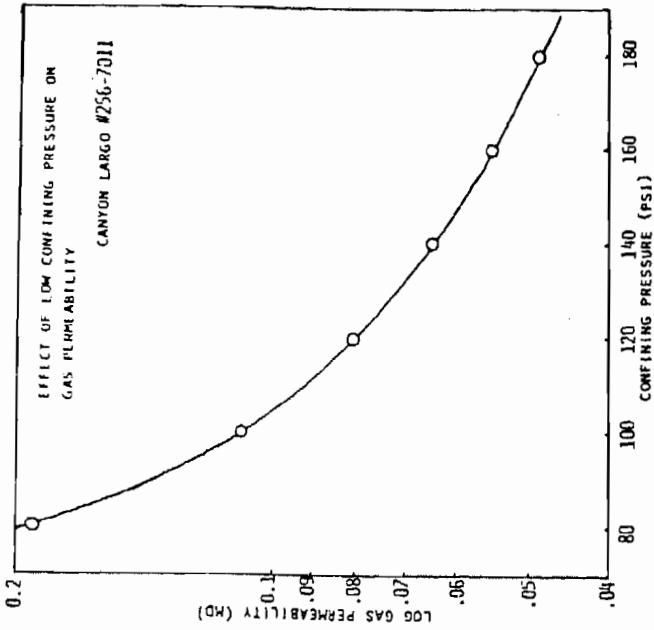


FIGURE 3

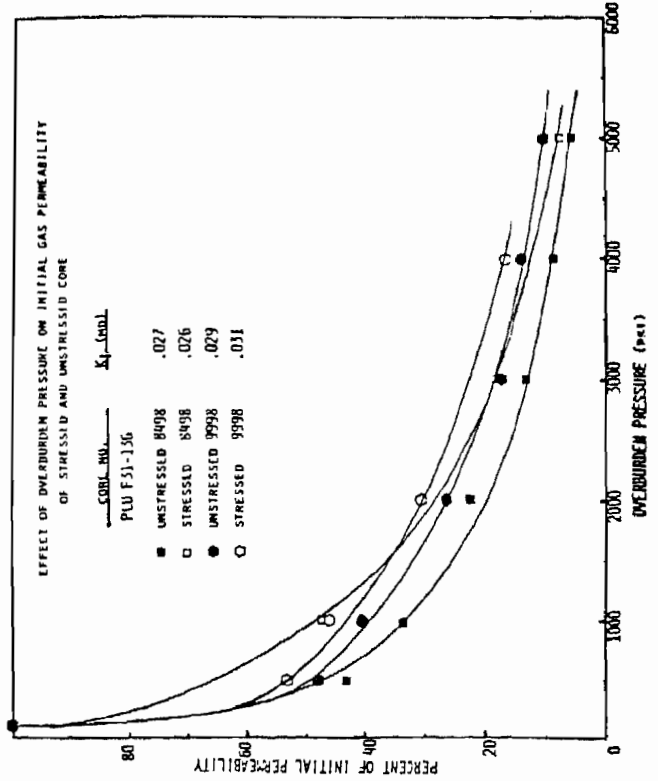


FIGURE 5

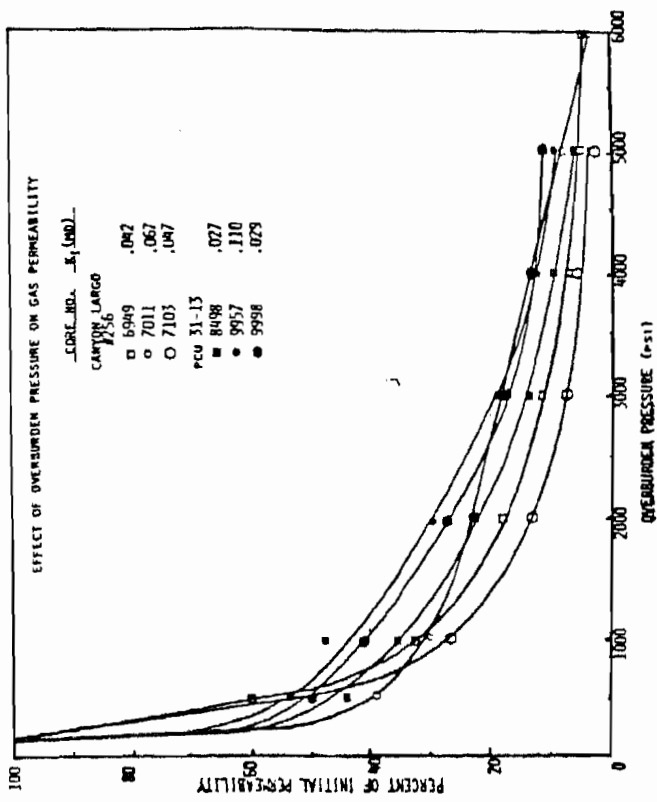


FIGURE 2

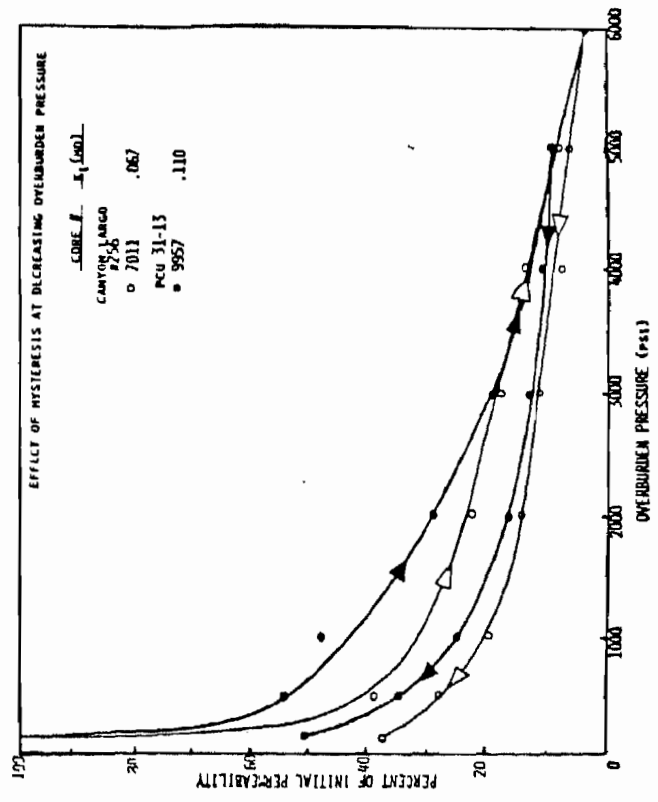


FIGURE 4

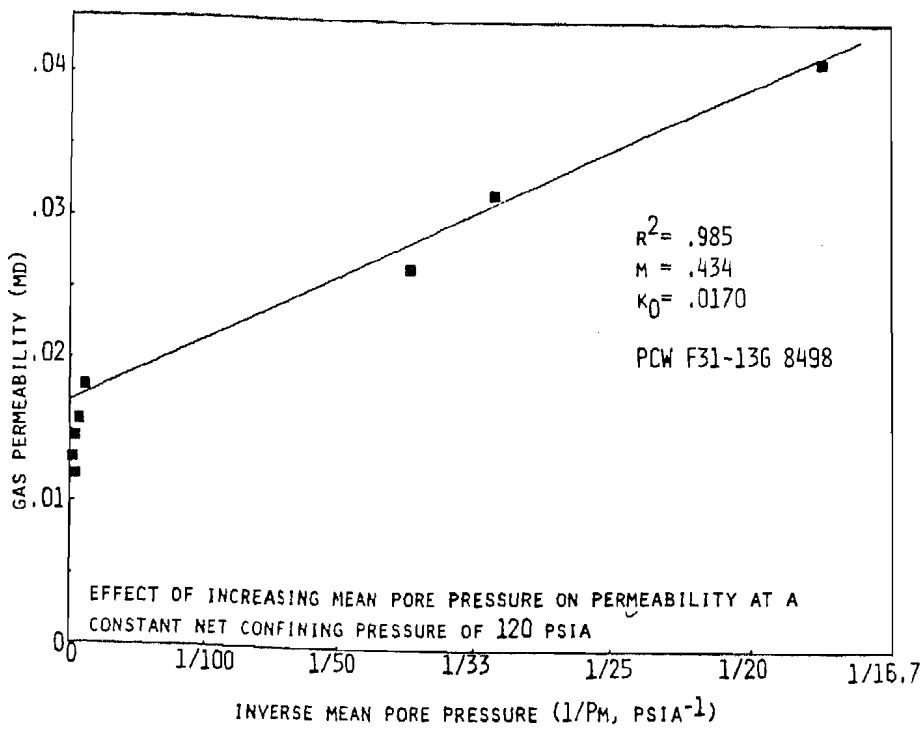


FIGURE 6

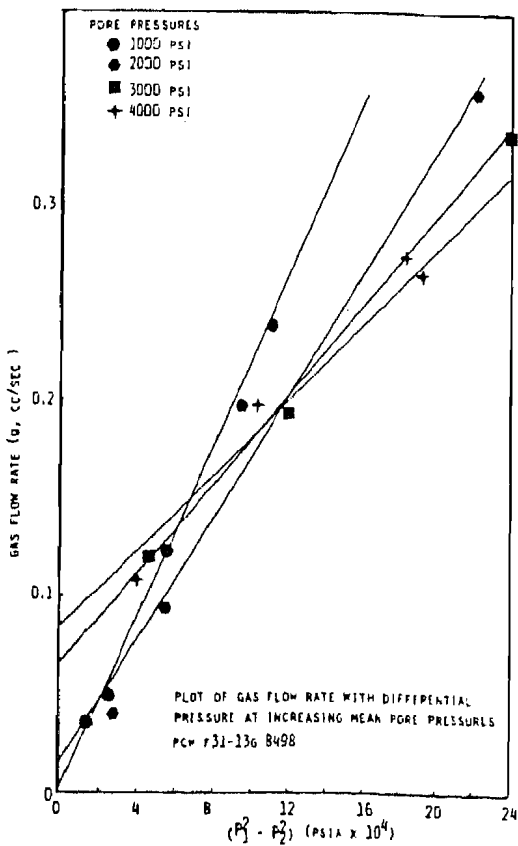


FIGURE 7

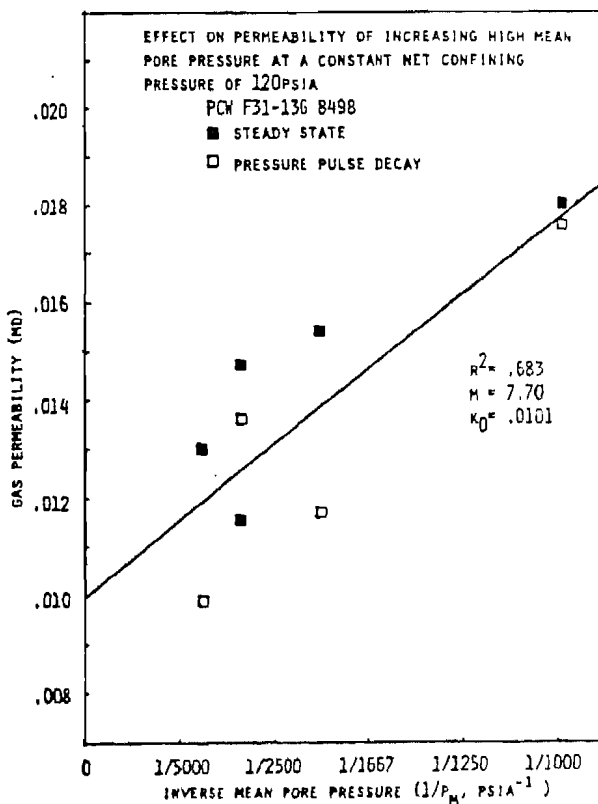


FIGURE 8

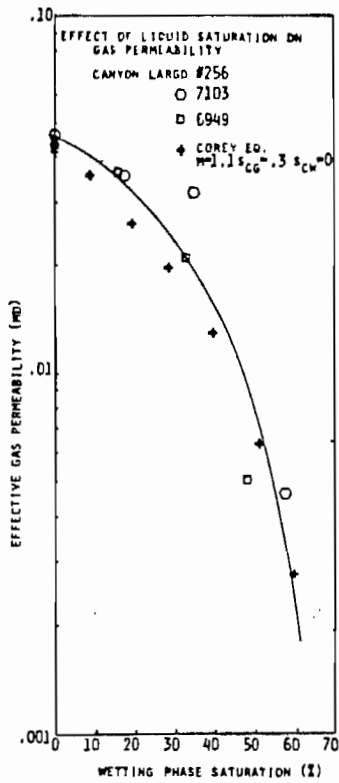


FIGURE 9

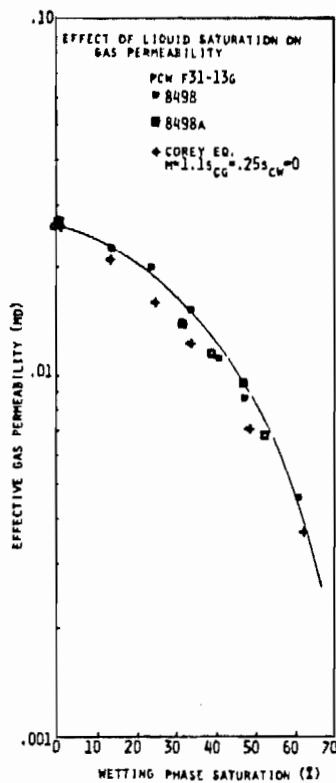


FIGURE 10

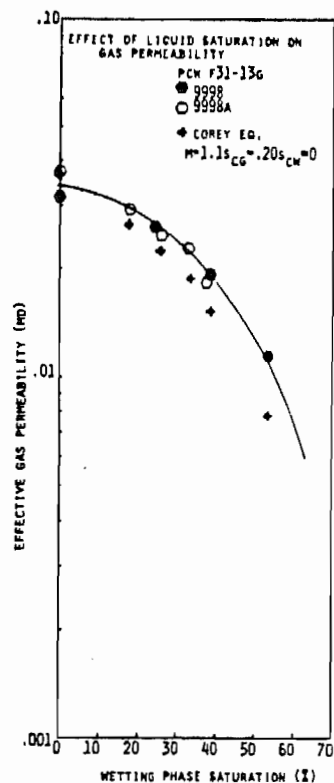


FIGURE 11

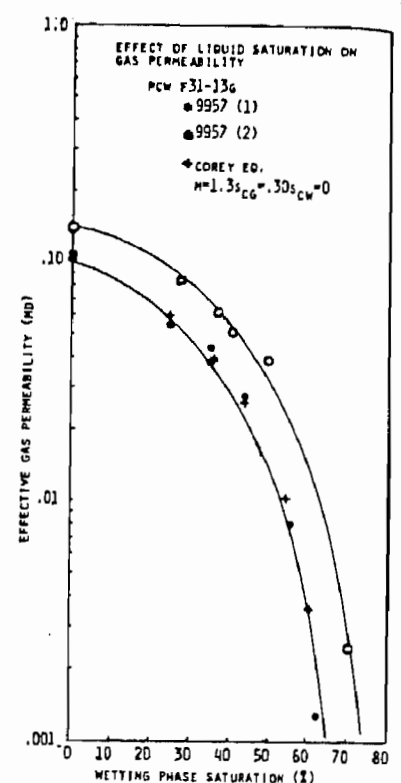


FIGURE 12

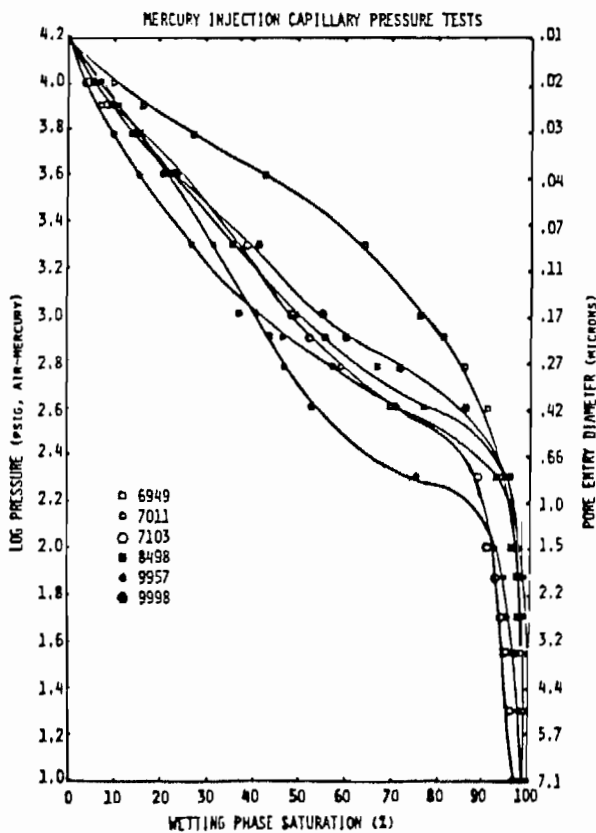


FIGURE 13

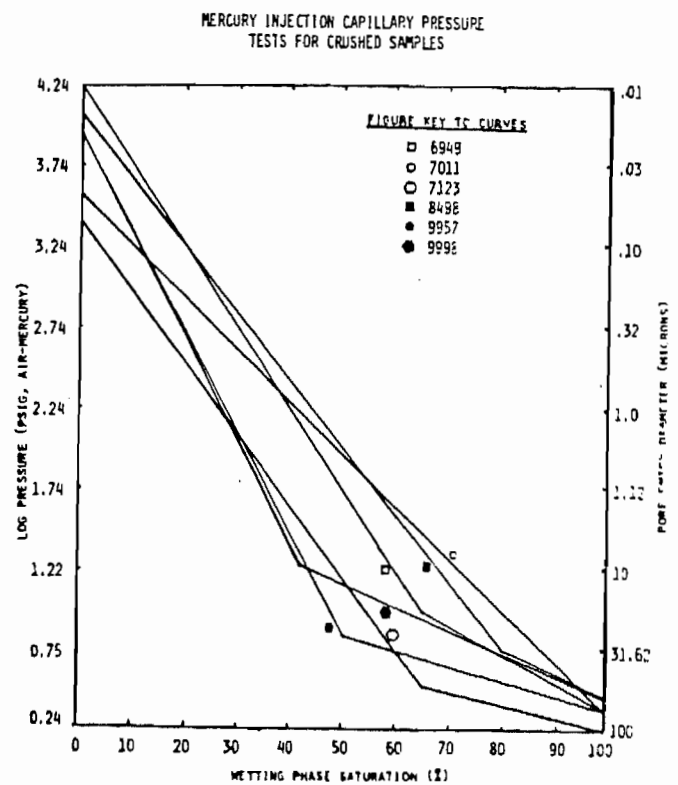


FIGURE 14

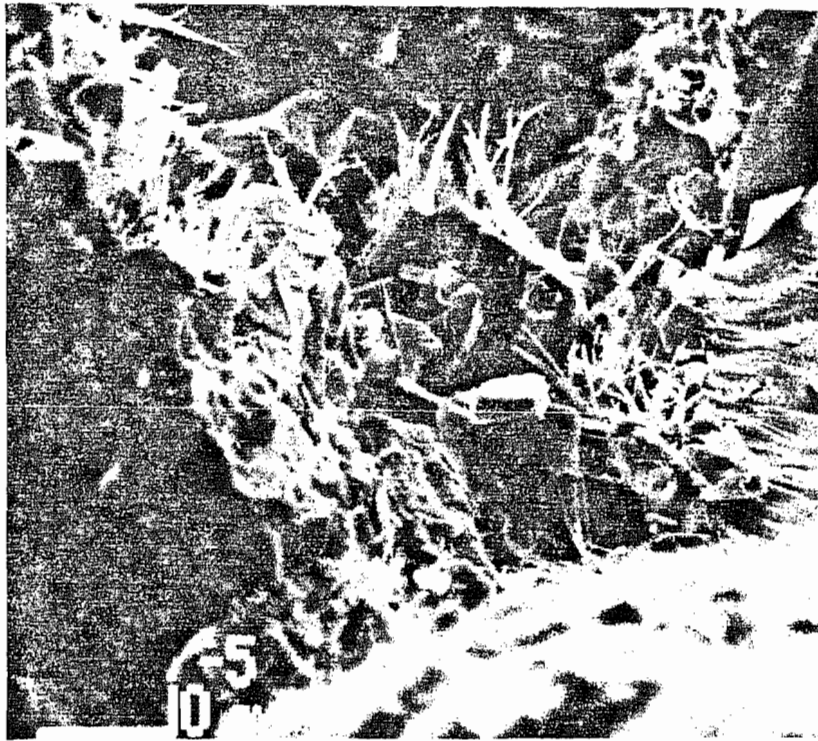


FIGURE 17. MOBIL F31-136-9957, 1200X, AUTHIGENIC ILLITE COATING DETRITAL QUARTZ AND FELDSPAR, NOTE EUHEDRAL QUARTZ GRAIN INDICATING DIAGENETIC PERIOD OF QUARTZ PRECIPITATION

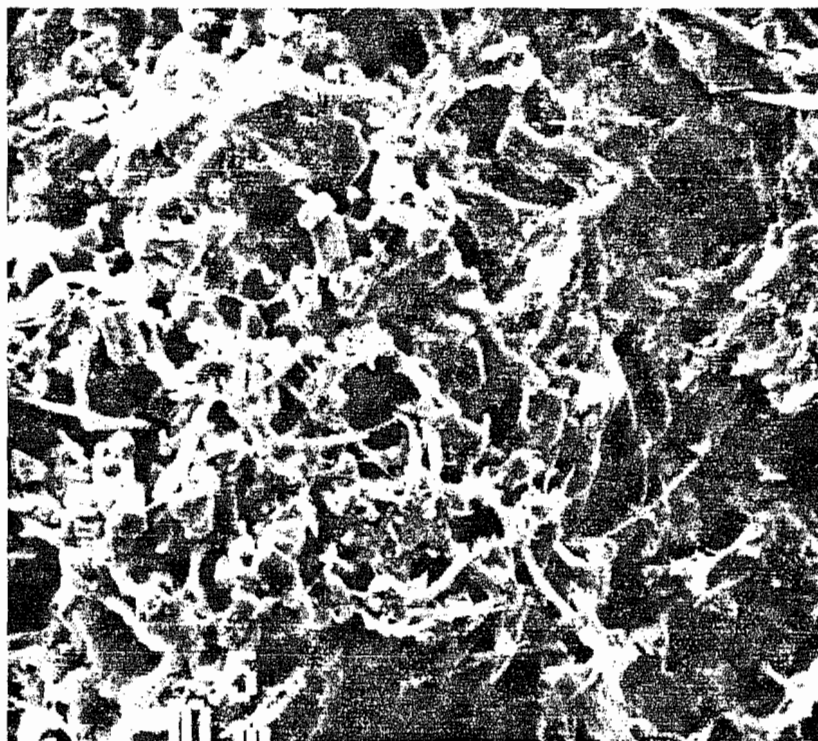


FIGURE 18. MOBIL F31-136-9957, 1200X, CLAY SURFACES AFTER IMMERSION IN 60,000 PPM NaCl SOLUTION, NOTE CEMENTATION NOT APPARENT IN FIGURE 17 INDICATING LIMITED SOLUTION ROCK INTERACTION

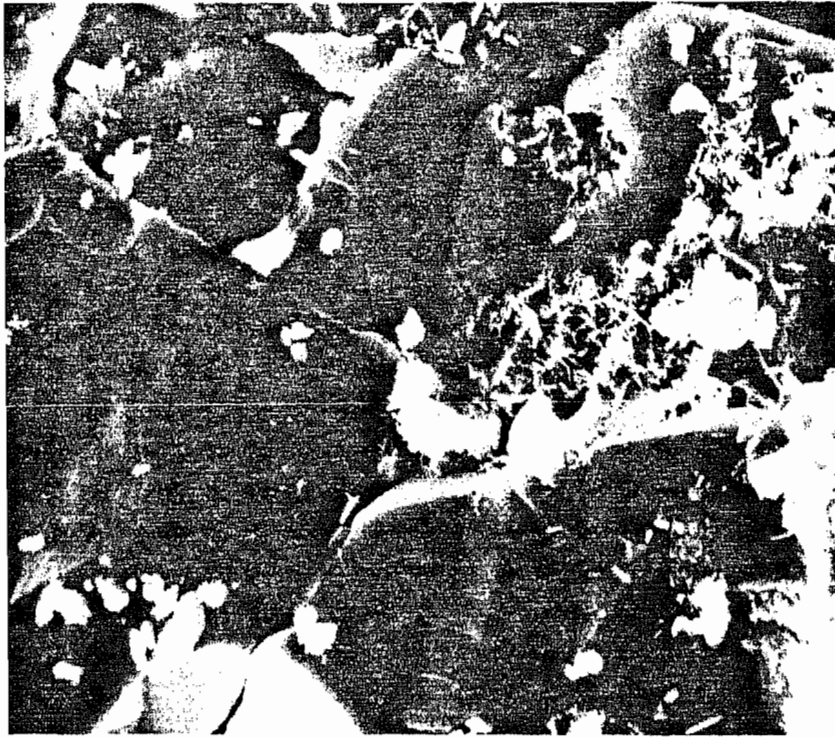


FIGURE 15. CANYON LARGO #256-7011, 1150X, $1.7 \text{ CM} = 10^{-5} \text{ MT}$,
DISPLAYS AUTHIGENIC ILLITE CLAY COATING DETRITAL GRAINS AND
LINING PORES

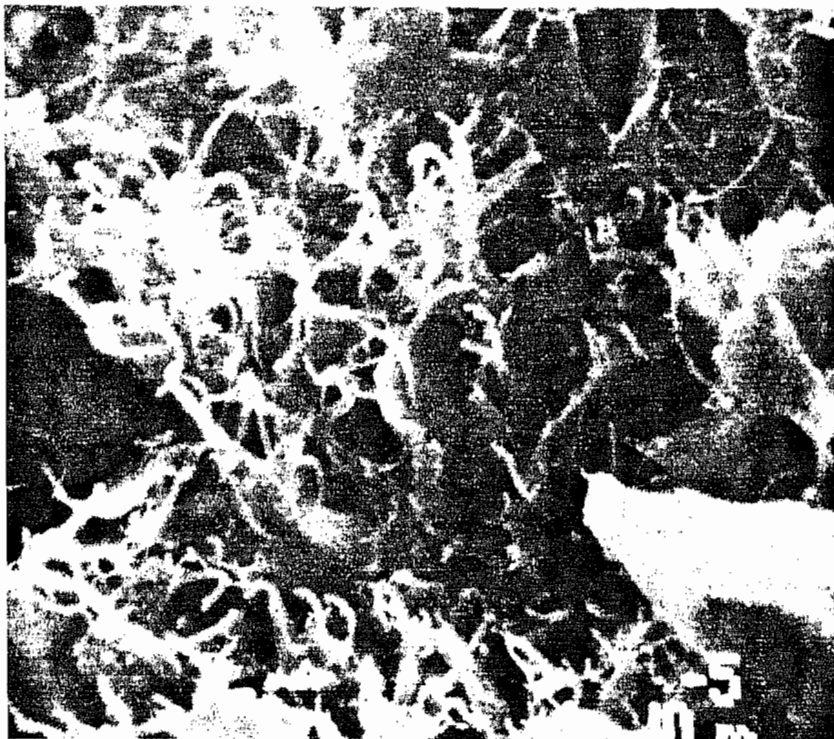


FIGURE 16. CANYON LARGO #256-7011, 5750X, HIGHER
MAGNIFICATION OF FIGURE 15 ILLUSTRATES FRAGILE MICROPOROUS
NETWORK IN PORE ENTRY